Radiation Measurements 132 (2020) 106248

Contents lists available at ScienceDirect

Radiation Measurements

journal homepage: http://www.elsevier.com/locate/radmeas

Design of a multi-shell portable neutron spectrometry system based on indium foil detectors

Alvie Asuncion-Astronomo [a,*], Frederick C. Hila [b], Cheri Anne M. Dingle [b], Charlotte V. Balderas [b], Rafael Miguel M. Dela Cruz [a], Neil Raymund D. Guillermo [b]

[a] Nuclear Reactor Operations Section, Philippine Nuclear Research Institute – DOST, Diliman, Quezon City, 1101, Philippines
[b] Applied Physics Research Section, Philippine Nuclear Research Institute – DOST, Diliman, Quezon City, 1101, Philippines

ARTICLE INFO

Keywords:
Response function
MCNP
Neutron spectrometry
Bonner spheres

ABSTRACT

A portable neutron spectrometry system was designed based on thermal neutron detectors embedded in concentric polyethylene spherical shells. The system is flexible and can accommodate the use of either active or passive neutron detectors in different configurations. In this work, the response matrix of the system with In-115 foil detectors was calculated with MCNP5 v.1.6. Activation foils were chosen as an ideal detector for the planned use of the system in medical accelerator environments. Calculations were performed using ENDF/B VII.0 and ENDF/B VIII.0 data libraries. The response functions calculated with the two libraries differ by as much as 11.6% in the thermal energy region for the largest moderator. A sensitivity analysis was also performed to evaluate the effect of main design parameters on the response matrix.

1. Introduction

Neutrons exhibit unique properties that make them ideal for numerous applications in fields like environment and agricultural research, biomedical research, nanotechnology, material science, and nuclear physics (Kardjilov et al., 2018), (Fragneto et al., 2018). Understanding these particles are also essential in the operation of fission reactors and in the development of fusion reactors and new fission reactors (Goričanec et al., 2018; Häußler et al., 2018; Pérez et al., 2019). In the medical sector, linear accelerators (LINACs) and positron emission tomography (PET) cyclotrons produce neutrons as a byproduct (Karimi et al., 2019; Khabaz, 2018; Vichi et al., 2019). These applications require the characterization of neutron fields to evaluate the potential neutron dose to radiation workers and the public. However, neutron fluence-to-dose conversion coefficients are largely dependent on neutron energy. It is thus essential to determine the neutron spectrum to ensure that dose from neutrons are properly evaluated.

The most widely used neutron spectrometer is the Bonner sphere spectrometer (BSS), which consists of a thermal neutron detector embedded in the center of polyethylene (PE) spheres with different diameters (Bramblett et al., 1960). Neutron moderation in the PE spheres depends on the incident neutron energy and the size of the sphere. Therefore, several different-diameter moderating spheres are required for a BSS system to resolve the energy distribution of neutrons in a given location. Due to the number of required spheres and its high density, conventional Bonner spheres tend to be bulky, heavy, and challenging to use in field measurements. However, BSS remains to be the standard device used in neutron spectrometry due to its isotropic response and sensitivity to neutrons over a broad range (Thomas and Alevra, 2002).

Several studies proposed alternative configurations of moderator sets and thermal neutron detector. These include the use of cylindrical PE moderators (Ghal–Eh et al., 2017; Gómez-Ros et al., 2015; Liamsuwan et al., 2018) that are ideal for collimated neutron fields. Nested moderator configurations (Liamsuwan et al., 2018), (Dubeau et al., 2012) and multiple detectors embedded in a moderator (Gómez-Ros et al., 2010), (Gómez-Ros et al., 2012) were likewise designed to provide a more compact alternative to BSS. Various options are also available for the thermal neutron detectors to be embedded in the moderators. Active neutron detectors such as $^{10}BF_3$ and ^{3}He proportional counters, and ^{6}LiI (Eu) scintillators have been used that can perform real-time measurements (Thomas and Alevra, 2002). However, these detectors are vulnerable to dead-time losses, pulse pile-up and electromagnetic interferences that are typical in LINACs, PET cyclotrons, and other intense radiation fields (Vega-Carrillo et al., 2014). Passive neutron detectors provide a better alternative in these harsh environments. Passive detectors also have the additional advantage of reduced cost, low

* Corresponding author.
E-mail address: ajasuncion@pnri.dost.gov.ph (A. Asuncion-Astronomo).

https://doi.org/10.1016/j.radmeas.2020.106248
Received 29 June 2019; Received in revised form 19 November 2019; Accepted 22 January 2020
Available online 23 January 2020
1350-4487/© 2020 Elsevier Ltd. All rights reserved.

sensitivity to gamma radiation, and versatility due to its ability to work even in harsh environments. Neutron detectors that have been used in passive systems include thermoluminescent dosimeters (TLDs) and activation foils such as gold, indium and dysprosium (Vega-Carrillo et al., 2014; Vlk and Pavlovič, 2018; Fernández et al., 2007; Bedogni et al., 2013).

The Philippine Nuclear Research Institute (PNRI) is establishing a neutron laboratory and a subcritical reactor assembly (Asuncion-Astronomo et al., 2019) as part of capacity building activities in nuclear science and technology. In support of these projects, a portable neutron spectrometry system (PNSS) has been designed, which consists of concentric PE spherical shells. The shells can be assembled to match solid PE spheres with 10 different diameters and can accommodate both passive and active neutron detectors. In this work, the response matrix of the PNSS with a central indium foil neutron detector is calculated using MCNP5 v.1.6 (X-5 Monte Carlo Team, 2003) to determine the response of the system in different neutron fields. Calculations were performed using the recently released ENDF/B VIII.0 nuclear data library (Brown et al., 2018) and the well-validated ENDF/B VII.0 (Chadwick et al., 2006) to compare the response matrices obtained with different nuclear data libraries. The effects of variations in the PE density and dimensions on the calculated response matrix were likewise investigated and discussed. Moreover, anisotropy effect was quantified for the smallest moderator of the PNSS.

2. Materials and methods

2.1. Design of the portable neutron spectrometry system (PNSS)

The portable neutron spectrometry system (PNSS) consists of one small sphere (∅ 5 cm) and nine spherical moderator shells that are divided into hemispheres. Table 1 summarizes the dimensions of the PE moderators comprising the PNSS with tolerances of $\pm$ 0.002 cm. Each moderator is designed to fit into the next shell which can provide different moderator thickness by adding the succeeding shells. The sphere and all the shells have cylindrical perforations (∅ 1.5 cm) across its center as illustrated in Fig. 1. These perforations can accommodate both active and passive neutron detectors and can be plugged with cylindrical PEs when not in use. An aluminum support assembly is also included in the design to serve as the support base of the spheres. The height of the support assembly can be adjusted to allow flexibility in the vertical positioning of the spheres.

The design of PNSS offers different possible arrangements for the thermal neutron detector. A cylindrical active detector with diameter $\leq$ 1.5 cm can fit in the sphere's perforations as illustrated in Fig. 2a. Multiple activation detectors can also be embedded at different locations in the shells (Fig. 2b), which is similar to the proposed single-sphere neutron spectrometer (Gómez-Ros et al., 2010), (Gómez-Ros et al., 2012). However, the focus of this work is the typical detector-moderator configuration illustrated in Fig. 2c, where an activation foil detector is embedded at the center of the spheres by securing it with the PE plugs. This configuration has been chosen because several studies (Amgarou and Lacoste, 2010; Bedogni et al., 2008; Fernandez et al., 2007) are available that can be used as a basis of comparison for the current work, while a foil detector is preferred since PNSS will be deployed in LINACs and PET cyclotrons.

Table 1
Dimensions of the PNSS polyethylene moderators.

Sphere/shell label	Internal diameter (cm)	External Diameter (cm)
5.0	N/A	4.995 $\pm$ 0.002
6.5	5.005 $\pm$ 0.002	6.495 $\pm$ 0.002
8.0	6.505 $\pm$ 0.002	7.995 $\pm$ 0.002
9.5	8.005 $\pm$ 0.002	9.495 $\pm$ 0.002
11.0	9.505 $\pm$ 0.002	10.990 $\pm$ 0.002
13.0	11.005 $\pm$ 0.002	12.990 $\pm$ 0.002
16.0	13.005 $\pm$ 0.002	15.990 $\pm$ 0.002
20.0	16.005 $\pm$ 0.002	19.990 $\pm$ 0.002
25.0	20.005 $\pm$ 0.002	24.990 $\pm$ 0.002
30.0	25.005 $\pm$ 0.002	30.000 $\pm$ 0.002

Indium activation foil detectors will be employed with the PNSS moderators. Indium has been effectively used in passive neutron spectrometers as demonstrated in a dual foil Bonner sphere extended system (Wang et al., 2010) and, recently, in a multi-sphere spectrometer (Vlk and Pavlovič, 2018). However, there is still limited literature on In-based BSS and this present work aims to further establish the use of this material in neutron spectrometry. An indium foil is composed of ^{113}In (4.29%) and ^{115}In (95.71%) nuclides with thermal neutron capture cross sections (σ_{th}) of 12 b and 202 b, respectively.[1] Due to its higher abundance and cross section, this study only accounts for neutron activation products from ^{115}In. Compared to ^{197}Au-197 (σ_{th} = 98.65 b), which is more commonly used with passive systems, ^{115}In has the following advantages: (1) it has higher thermal neutron absorption cross section ($\sim$202 b); (2) its relevant activation product, ^{116m1}In, has a short half-life at 54 min, which means shorter saturation time; (3) it is cheaper and more abundant than gold (Vlk and Pavlovič, 2018). These characteristics are ideal for the planned utilization of PNSS in accelerator environments which offers limited irradiation time.

2.2. Monte Carlo calculation of the response matrix

Fig. 3 shows the model of the PNSS geometry that was prepared based on the dimensions of the PE spheres (ρ = 0.939 g cm^{-3}) listed in Table 1. The geometry of the model allowed easier implementation of the Russian roulette variance reduction method, where the neutron importance of each cell is gradually increased towards the tally region. The indium foil (ρ = 7.31 g cm^{-3}) was modeled at the center of the moderators, as a disc with a diameter of 1.27 cm and thickness of 0.127 mm and oriented perpendicular to the source. The source is defined as a disc with the same diameter as the PE sphere combination that is simulated.

Each foil-moderator combination has a response function $R_i(E)$ that is defined as the number of radiative capture (n,γ) reactions in the indium foil per unit neutron fluence rate per unit indium mass. The PNSS response matrix is the set of $R_i(E)$ for all the PE spheres comprising the system. Following the method described in (Amgarou and Lacoste, 2010), $R_i(E)$ was calculated using the F4 tally and the FM card in MCNP:

$$R_i(E) = \frac{NA_i}{\rho} \int \varphi(E)\sigma_E(\mathrm{n},\gamma)dE \tag{1}$$

In equation (1), N is the atom density (cm^{-3}), $A_i = \pi r_i^2$ is the surface area of the source that was chosen to match the radius of the irradiated sphere r_i, ρ is the density of the indium foil (7.31 g cm^{-3}), $\varphi(E)$ is the fluence per energy bin that is estimated by the F4 tally in units of cm^{-2}, and $\sigma_E(\mathrm{n},\gamma)$ is the corresponding cross section per energy bin for the (n,γ) reaction in units of barn (10^{-24} cm^2). The resulting quantity is multiplied by 0.79 to take into account the yield of the ^{116m1}In nuclide produced by ^{115}In(n,γ)^{116m1}In reactions, which accounts for 79% of the total neutron interaction with indium. Dimension analysis shows that the unit of $R(E)$ is cm^2 g^{-1}.

The PNSS response functions were calculated for incident neutron energy range of 1 meV–100 MeV divided into 120 equidistant logarithmic intervals. Calculations of $R(E)$ are performed with MCNP5v.1.6 code (X-5 Monte Carlo Team, 2003) using a computer with 32 cores, 64 threads and 3.00 GHz processors. 60 threads were used to allow parallel

[1] IAEA Nuclear Data Services at https://www-nds.iaea.org/(23 May 2019, date last accessed).

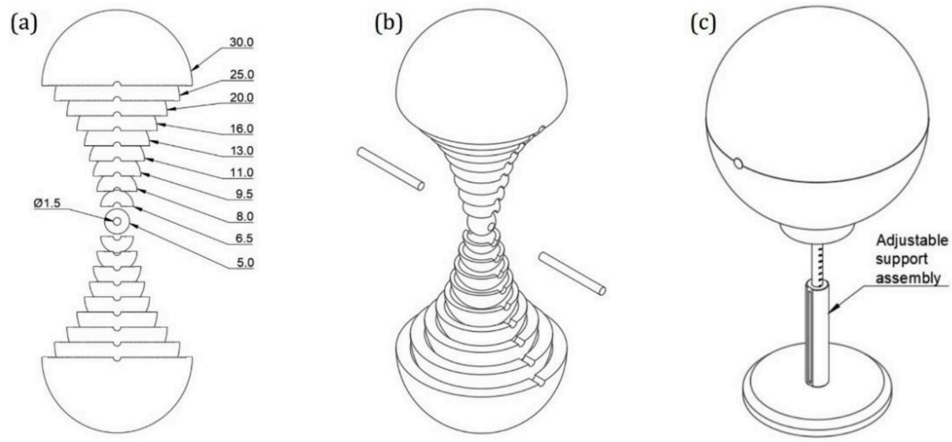

Fig. 1. Design for concentric spherical shell polyethylene moderators in exploded (a) front and (b) isometric view. (c) Assembled PNSS with aluminum support assembly.

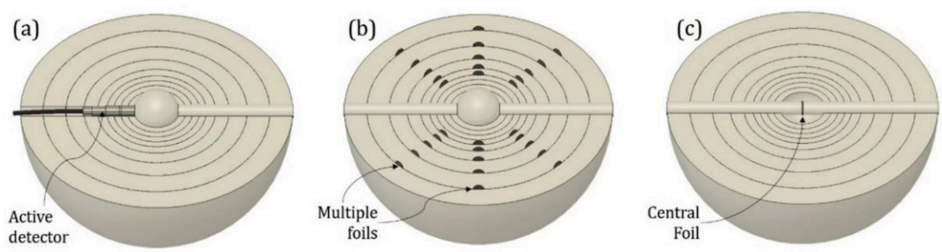

Fig. 2. Different arrangements of thermal neutron detector in the PNSS: (a) active detector-moderator system; (b) multiple foil detector-moderator system; (c) central foil detector-moderator system. Top hemisphere of PNSS removed to illustrate location of detectors in the arrangement.

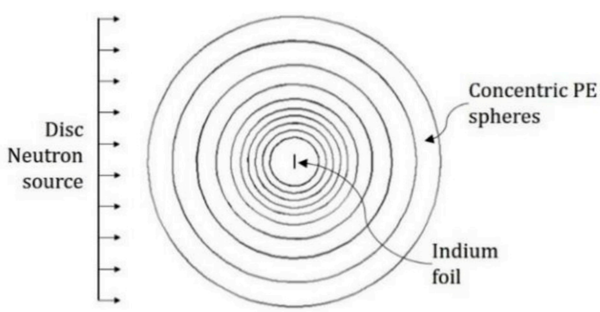

Fig. 3. Monte Carlo model used to simulate the PNSS response.

processing of each input file. The number of histories was chosen to keep statistical uncertainties lower than 0.5%. To reduce calculation time, the SCX feature of MCNP has been used, which allows binning of tallies. Source probability biasing was also implemented in addition to the Russian roulette variance reduction method.

All calculations have been performed using the most recent cross section data library available, ENDF/B VIII.0 and the corresponding thermal neutron scattering data S(α,β) (Brown et al., 2018). For comparison, calculations were also performed with the ENDF/B VII.0, which is a well-validated nuclear data library and the basis of response matrix calculations in previous studies. The effect of variations in relevant PNSS design parameters on the response matrix were also calculated. This includes changes in PE density as well as changes in the dimensions of the spherical shells. The isotropy of the response matrix was likewise investigated under different configurations of neutron incidence.

3. Results and discussion

3.1. PNSS response matrix

The calculated $R_i(E)$ for each moderator-foil configuration comprising the PNSS response matrix are plotted in Fig. 4. The plot peaks shift from the eV to the MeV neutron energy region with increasing moderator thickness, which demonstrates that PNSS can be used over a large neutron energy range. The sharp peak observed in the plot for the 5.0 cm sphere is due to the radiative capture resonance peak of indium in the 0.5 eV–3 eV range (Brown et al., 2018). On the other hand, the $R(E)$ plots for the 25.0 cm and 30.0 cm spheres display sharp dips in the 1–10 MeV region due to nuclear resonances of carbon in this energy range. These results are similar with those that are previously reported for passive BSS systems (Vlk and Pavlovič, 2018), (Amgarou and Lacoste, 2010; Bedogni et al., 2008; Fernandez et al., 2007).

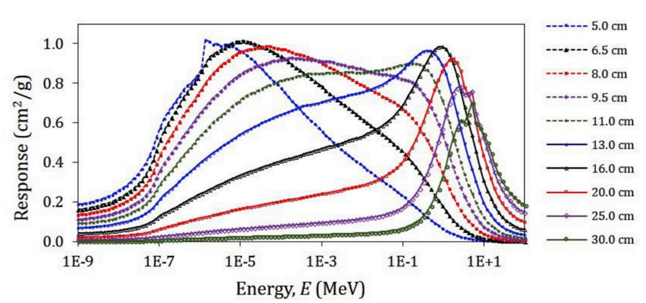

Fig. 4. Calculated response matrix of PNSS with a central indium foil detector. Statistical uncertainties are less than 0.5%.

3.2. Effect of nuclear data library

The most recent release of evaluated nuclear data library, ENDF/B-VIII.0 (ENDF8), features improved thermal neutron scattering data, S (α, β), for polyethylene and new evaluated data for neutron reactions with ^{1}H and carbon isotopes (Brown et al., 2018). Since most literature on BSS response matrices use the previous ENDF/B-VII.0 (ENDF7) library, the possible influence of the new library on the response functions has been investigated. The response functions of the PNSS spheres were recalculated using ENDF7, and the result was compared to those obtained with ENDF8 by calculating the percent difference. Fig. 5 provides a summary of the comparisons made for results obtained for the 5.0, 9.5, 16.0 and 30.0 cm spheres. The calculated percent difference between ENDF8 and ENDF7 response functions were also plotted.

Results show that the ENDF7 library tends to overestimate the response function compared to ENDF8. This is particularly evident for thermal neutrons and the effect becomes more significant with larger moderators. In the thermal energy region, the calculated response functions for the 5.0 cm sphere differ by as much as 4.71% while for the 30.0 cm sphere ENDF8 results are lower by as much as 11.6%. The deviation is due to the updated neutron scattering laws applied in ENDF8, which results in lower total cross section of PE for low energy neutrons. Compared to ENDF7, the S(α,β) data for PE that is included in ENDF8 is shown to have better agreement with experiment data (Brown et al., 2018), (Lavelle et al., 2013). In the high energy region of the plots, ENDF8 results are also slightly lower than ENDF7 results. This is attributed to the isotopic carbon evaluations that is incorporated in ENDF8 libraries while previous nuclear data libraries employ natural carbon evaluations (Brown et al., 2018), (Chadwick et al., 2006).

3.3. Effect of polyethylene density

The PE density used in the MCNP simulations is 0.939 g/cm^3, which is based on measured dimensions and masses of available PE plugs. To account for uncertainties in the PE density, the response functions with density variations of 0.939 g/cm^3 ± 0.005 g/cm^3 were calculated and the results were compared with the reference density.

The response functions corresponding to different PE densities and the calculated percent differences are plotted in Fig. 6 for the 5.0, 9.5, 16.0 and 30.0 cm spheres. The plots show that low density PE moderators result in higher response to neutrons with low energy compared to high density PE moderators. This trend is gradually reversed as the incident neutron energy is increased, and as evident in Fig. 6, the percent difference plots tend to cross at neutron energies that match the peaks of the response functions. Since the central indium foil is more sensitive to thermal neutrons, incident neutrons on the moderator-foil assembly should be thermalized for it to have higher reaction probability with the indium detector. Thus, low density PEs result in higher

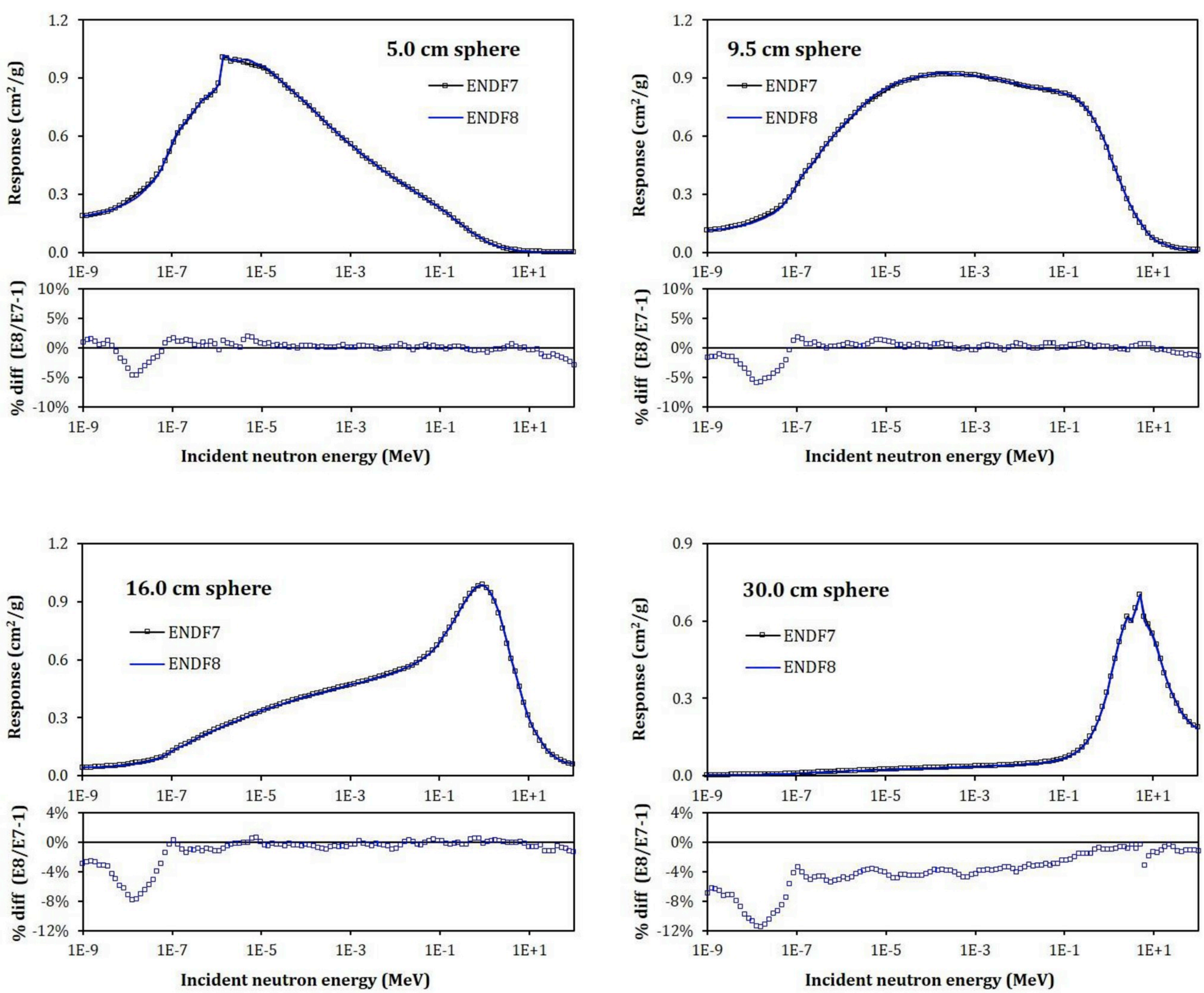

Fig. 5. Effect of the nuclear data library on the response function for representative PNSS spheres. The propagated uncertainties for the calculated percent difference are less than 1%.

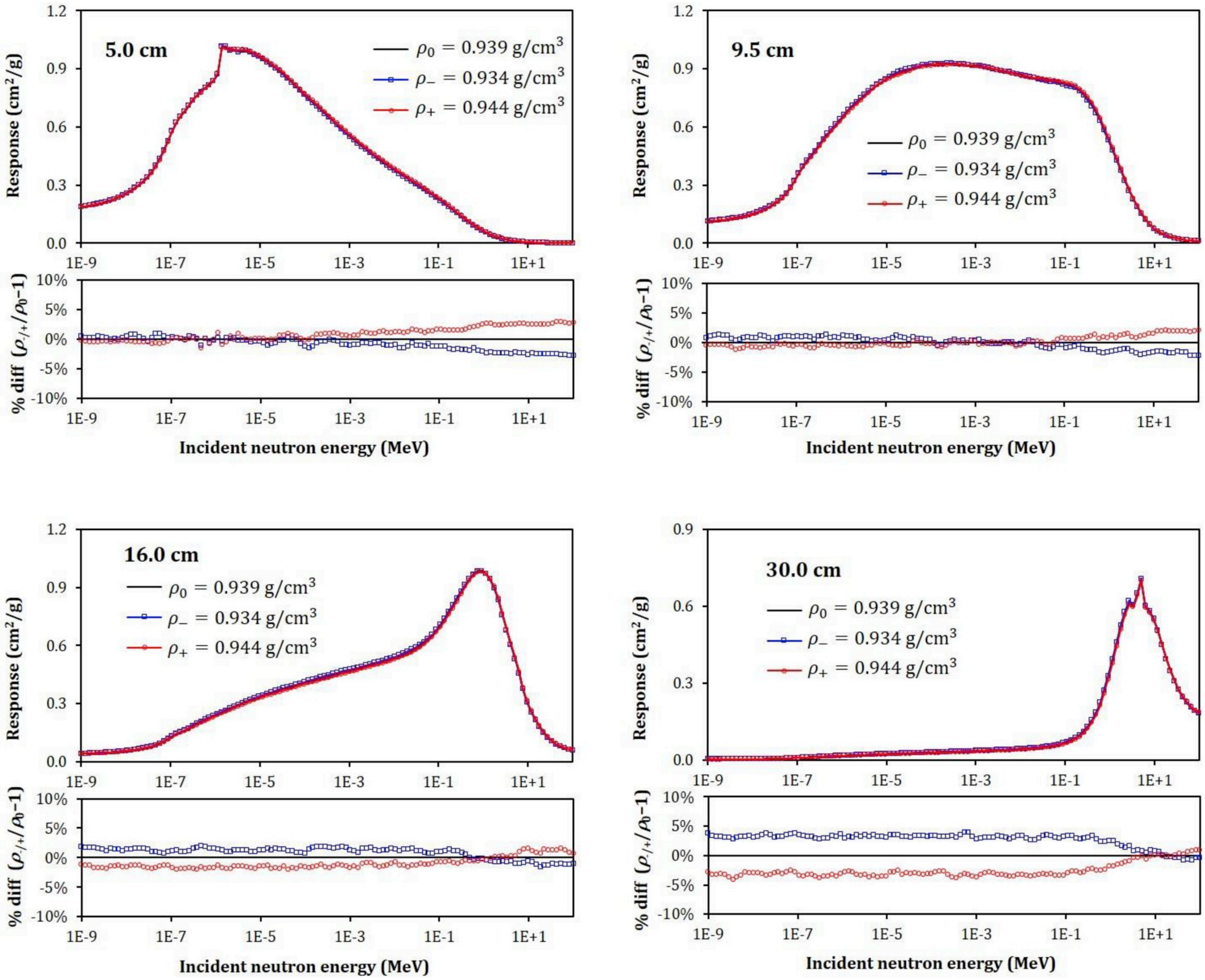

Fig. 6. Effect of variation on polyethylene density on the response function for representative PNSS spheres. The propagated uncertainties for the calculated percent difference are less than 1%.

interaction probability between indium and incident neutrons that already have low energy. This is observed up to the peaks of the response functions where neutrons have been optimally thermalized by the available moderator. For high density PEs, high energy neutrons have better chances of interacting with indium after the optimal thermalization. However, these mechanisms can be neglected for small density variations. For the considered densities, the highest percent differences that were calculated are 2.88% and 4.16% for the 5.0 cm and 30.0 cm spheres, respectively. As expected, changes in density have greater influence on larger moderators. It should be noted as well that the percent difference is minimal in the region where the response function peaks, which is more important in the evaluation of the neutron spectra.

3.4. Effect of gaps between PE spherical shells

Actual fabrication conditions of the PNSS spherical shells may result in gaps between adjacent shells that could affect neutron moderation. To investigate the effect of the gaps, we calculated the response functions for the PNSS with maximum gaps based on the expected uncertainties in the sphere dimensions at $\pm$ 0.002 cm. We also considered a test gap size of 0.02 cm that is one order of magnitude greater than the expected uncertainty. The PNSS response functions obtained with these gap sizes were then compared to the minimum gap size that is based on the PNSS spheres' dimensions as listed in Table 1.

The plots of response functions for the 6.5, 9.5, 16.0 and 30.0 cm spheres with three gap sizes are presented in Fig. 7. It is evident that the maximum gap size based on expected fabrication tolerances does not have significant effect on the response matrix of the PNSS. The maximum calculated deviations in the response functions are 0.77% for the 6.5 cm sphere and 1.49% for the 30.0 cm sphere. The difference is higher for larger moderators since they consist of more shells that introduce additional gaps between shells. Deviations in the response functions are more evident with the test gap, with maximum values of 3.34% for the 6.5 cm sphere and 5.83% for the 30.0 cm spheres. However, these deviations are still small even with a large test gap size. The response function plots that were obtained with larger gap sizes display patterns that is similar to the plots for PEs with decreased density. This indicates that the effect of gaps between spheres on the response function can be accounted for in the simulation model either by explicitly including the gaps or by decreasing the declared density of the PE moderators.

3.5. Effect of neutron incidence

Bonner sphere spectrometers typically have isotropic responses to neutron fields due to the spherical symmetry of the PE moderators and the central detectors. However, since PNSS uses indium foil detectors with a disc geometry, the potential anisotropy of the system was investigated. This was performed by calculating the response functions for parallel neutron incidence and a truly isotropic geometry and comparing the results to normal neutron incidence. Considering that anisotropy effects have been studied previously for foil-based BSS

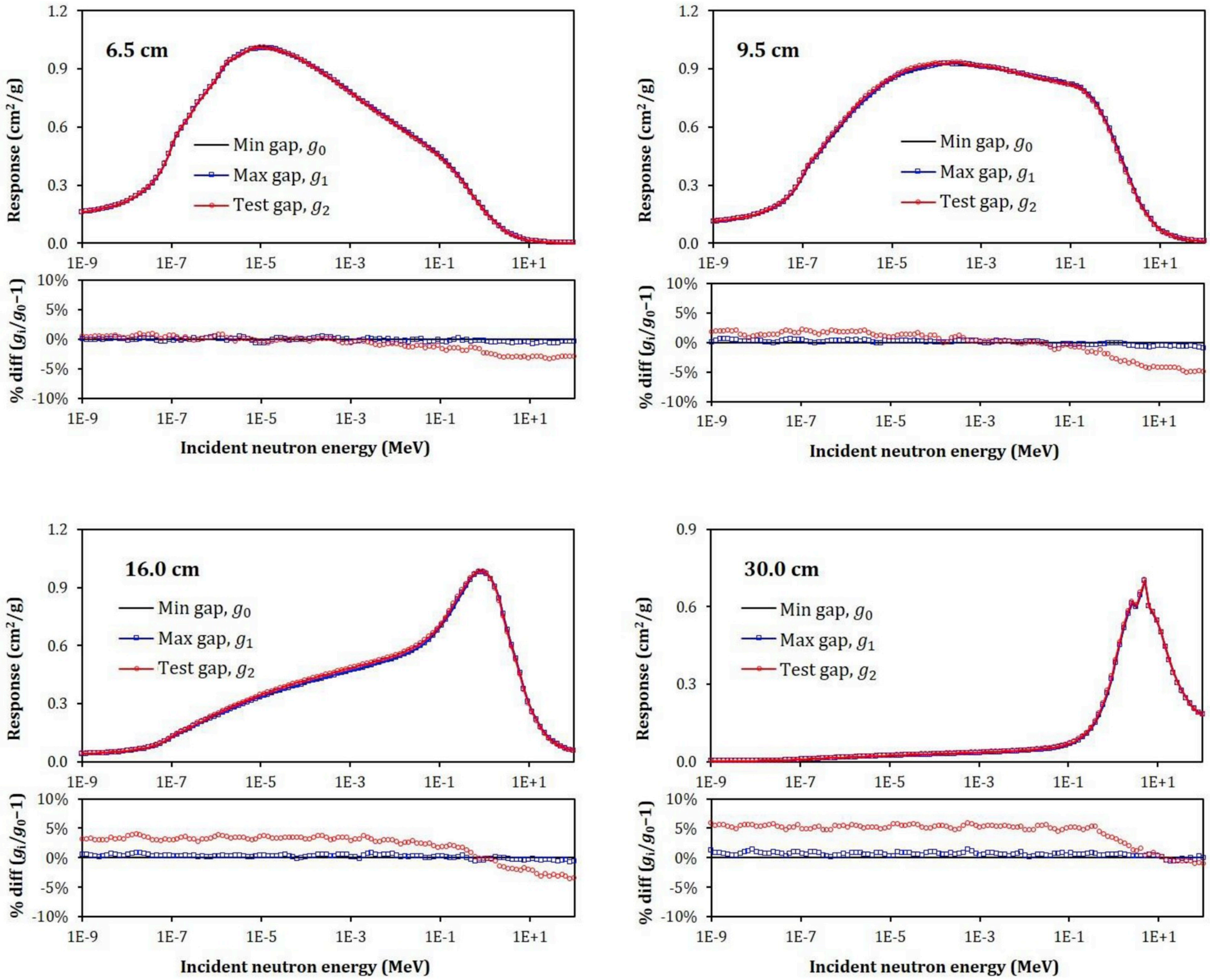

Fig. 7. Effect of gap between the PE shells on the response function for representative PNSS spheres. The propagated uncertainties for the calculated percent difference are less than 1%.

(Amgarou and Lacoste, 2010), (Fernandez et al., 2007), the current study only focused on the smallest and largest moderators of the PNSS.

The calculated result for the effect of neutron incidence on the response functions of the 5.0 and 30.0 cm spheres is shown in Fig. 8. The smallest moderator is more sensitive to anisotropy effects with calculated maximum deviations of 4.48% and 2.26% in the response function for parallel and isotropic incidences, respectively. On the other hand, the largest moderator appears to be immune to anisotropies with maximum deviations of 1.42% for parallel incidence and 1.74% for isotropic incidence. Larger moderators provide more scattering

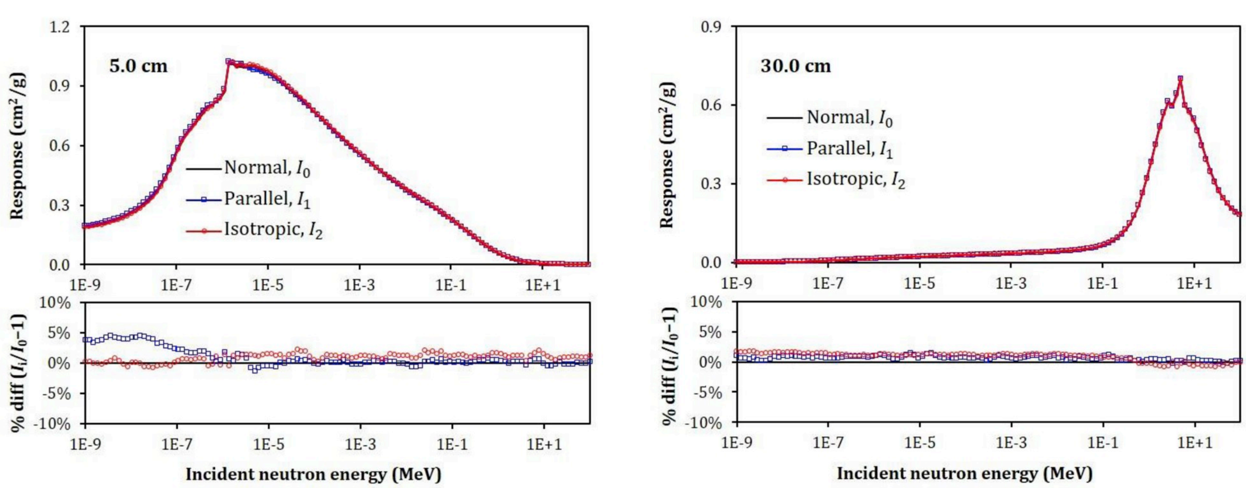

Fig. 8. Effect of the neutron incidence on the response function for representative PNSS spheres. The propagated uncertainties for the calculated percent difference are less than 1%.

materials for neutrons such that information on the source, including initial incidence, tends to be lost as the neutrons travel through the material. These results demonstrate that the presence of spherical PE moderators can adequately reduce effects of anisotropies on the PNSS.

4. Conclusion

A design for a portable neutron spectrometry system (PNSS) has been developed, which consists of concentric polyethylene shells that can accommodate thermal neutron detectors in different configurations. The use of indium as a passive central detector for the PNSS was investigated. The response matrix of the In-based PNSS for neutron energies from 1 meV to 10 MeV was calculated using MCNP5v1.6. Our results show that MCNP calculations with the newly released ENDF/B-VIII.0 library result in lower response for thermal neutrons compared to results obtained with the former ENDF/B-VII.0. This is due to the difference in the thermal scattering treatment that is employed by the nuclear data libraries. Moreover, the effect of main design parameters on the response functions of PNSS has been investigated. The parameters covered in the investigation include the variations in PE density, the size of gaps between the PE shells, and the direction of neutron incidence. Within a certain range, it is found that variations in these parameters have negligible effects on the PNSS response matrix. This work demonstrates that the PNSS provides an alternative compact configuration for Bonner sphere spectrometers.

Declaration of competing interest

The authors declare that they have no known competing financial interests or personal relationships that could have appeared to influence the work reported in this paper.

Acknowledgement

This work is funded by the Department of Science and Technology – Philippine Council for Industry, Energy and Emerging Technology Research and Development (DOST-PCIEERD) through the project "Development of a passive neutron spectrometry system" with Project No. 04385.

References

Amgarou, K., Lacoste, V., 2010. Response matrix evaluations of a passive Bonner sphere system used for neutron spectrometry at pulsed, intense and complex mixed fields. J. Instrum. 5 https://doi.org/10.1088/1748-0221/5/09/P09002 no. 09, p. P09002.

Asuncion-Astronomo, A., Štancar, Ž., Goričanec, T., Snoj, L., Apr. 2019. Computational design and characterization of a subcritical reactor assembly with TRIGA fuel. Nucl. Eng. Technol. 51 (2), 337–344.

Bedogni, R., Esposito, A., Gentile, A., Angelone, M., Gualdrini, G., Feb. 2008. Determination and validation of a response matrix for a passive Bonner sphere spectrometer based on gold foils. Radiat. Meas. 43 (2–6), 1104–1107.

Bedogni, R., et al., Jun. 2013. Testing a newly developed single-sphere neutron spectrometer in reference monochromatic fields from 147keV to 14.8MeV. Nucl. Instruments Methods Phys. Res. Sect. A Accel. Spectrometers, Detect. Assoc. Equip. 714, 110–114.

Bramblett, R.L., Ewing, R.I., Bonner, T.W., Oct. 1960. A new type of neutron spectrometer. Nucl. Instrum. Methods 9 (1), 1–12.

Brown, D.A., et al., 2018. ENDF/B-VIII.0: the 8thMajor release of the nuclear reaction data library with CIELO-project cross sections, new standards and thermal scattering data. Nucl. Data Sheets 148, 1–142.

Chadwick, M.B., et al., 2006. ENDF/B-VII.0: next generation evaluated nuclear data library for nuclear science and Technology. Nucl. Data Sheets 107 (12), 2931–3060.

Dubeau, J., Hakmana witharana, S.S., Atanackovic, J., Yonkeu, A., Archambault, J.P., 2012. A neutron spectrometer using nested moderators. Radiat. Protect. Dosim. 150 (2), 217–222.

Fernández, F., et al., 2007. Neutron spectrometry in a PET cyclotron with a Bonner sphere system. Radiat. Protect. Dosim. 126 (1–4), 371–375.

Fernandez, F., et al., 2007. Monte Carlo calculations and validation of a gold foil-based bonner sphere system. Radiat. Protect. Dosim. 126 (1–4), 366–370.

Fragneto, G., Delhom, R., Joly, L., Scoppola, E., Nov. 2018. Neutrons and model membranes: moving towards complexity. Curr. Opin. Colloid Interface Sci. 38, 108–121.

Ghal–Eh, N., Kalaei, M., Mohammadi, A., Vega–Carrillo, H.R., Oct. 2017. Replacement of Bonner spheres with polyethylene cylinders for the unfolding of an 241 Am–Be neutron energy spectrum. Appl. Radiat. Isot. 128 (April), 292–296.

Gómez-Ros, J.M., Bedogni, R., Moraleda, M., Delgado, A., Romero, A., Esposito, A., Jan. 2010. A multi-detector neutron spectrometer with nearly isotropic response for environmental and workplace monitoring. Nucl. Instruments Methods Phys. Res. Sect. A Accel. Spectrometers, Detect. Assoc. Equip. 613 (1), 127–133.

Gómez-Ros, J.M., et al., 2012. Designing an extended energy range single-sphere multi-detector neutron spectrometer. Nucl. Instruments Methods Phys. Res. Sect. A Accel. Spectrometers, Detect. Assoc. Equip. 677, 4–9.

Gómez-Ros, J.M., et al., Nov. 2015. CYSP: a new cylindrical directional neutron spectrometer. Conceptual design. Radiat. Meas. 82, 47–51.

Goričanec, T., et al., Jan. 2018. Evaluation of neutron flux and fission rate distributions inside the JSI TRIGA Mark II reactor using multiple in-core fission chambers. Ann. Nucl. Energy 111, 407–440.

Häußler, A., Warmer, F., Fischer, U., Nov. 2018. Neutronics analyses for a stellarator power reactor based on the HELIAS concept. Fusion Eng. Des. 136, 345–349.

Kardjilov, N., Manke, I., Woracek, R., Hilger, A., Banhart, J., Jul. 2018. Advances in neutron imaging. Mater. Today 21 (6), 652–672.

Karimi, A.H., Brkić, H., Shahbazi-Gahrouei, D., Haghighi, S.B., Jabbari, I., Mar. 2019. Essential considerations for accurate evaluation of photoneutron contamination in radiotherapy. Appl. Radiat. Isot. 145, 24–31.

Khabaz, R., Sep. 2018. Effect of each component of a LINAC therapy head on neutron and photon spectra. Appl. Radiat. Isot. 139, 40–45.

Lavelle, C.M., Liu, C.-Y., Stone, M.B., May 2013. Toward a new polyethylene scattering law determined using inelastic neutron scattering. Nucl. Instruments Methods Phys. Res. Sect. A Accel. Spectrometers, Detect. Assoc. Equip. 711, 166–179.

Liamsuwan, T., Channuie, J., Wonglee, S., Kowatari, M., Nishino, S., Aug. 2018. Characterization of an in-house developed multi-cylindrical moderator neutron spectrometer. Radiat. Protect. Dosim. 180 (1–4), 1–4.

Pérez, D.M., Lorenzo, D.E.M., de Oliveira Lira, C.A.B., Garcia, L.P.R., Jun. 2019. Neutronic evaluation of the steady-state operation of a 20 kWth Aqueous Homogeneous Reactor for Mo-99 production. Ann. Nucl. Energy 128, 148–159.

Thomas, D.J., Alevra, A.V., 2002. Bonner sphere spectrometers - a critical review. Nucl. Instruments Methods Phys. Res. Sect. A Accel. Spectrometers, Detect. Assoc. Equip. 476 (1–2), 12–20.

Vega-Carrillo, H.R., Guzman-Garcia, K.A., Gallego, E., Lorente, A., Oct. 2014. Passive neutron area monitor with pairs of TLDs as neutron detector. Radiat. Meas. 69, 30–34.

Vichi, S., et al., Aug. 2019. Activation studies of a PET cyclotron bunker. Radiat. Phys. Chem. 161, 48–54.

Vlk, P., Pavlovič, M., 2018. Calculation and validation of the response matrix for a neutron multisphere spectrometer with an indium central detector. Radiat. Protect. Dosim. 179 (1), 1–8.

Wang, Z., Howell, R.M., Burgett, E.A., Kry, S.F., Hertel, N.E., Salehpour, M., 2010. Calibration of indium response functions in an Au-In-BSE system up to 800 MeV. Radiat. Protect. Dosim. 139 (4), 565–573.

X-5 Monte Carlo Team, 2003. MCNP - A General Monte Carlo N-Particle Transport Code, Version 5. LA-CP-03-0245, LANL.